Folate-conjugated dually responsive micelles for targeted anticancer drug delivery

Lingling Zhao,*[ab] Yajuan Zhang,[a] Jia Shao,[a] Hongze Liang,[a] Haining Na*[b] and Jin Zhu*[b]

Phenylboronic acid and folate grafted chitosan hydrochloride (FHCSPBA) was synthesized and confirmed by FTIR and ^{1}H NMR. Glucose and pH dually responsive micelles were obtained through self-assembly of the amphiphilic polymers. The prepared FHCSPBA micelles displayed good biocompatibility and sustained drug release of the model drug doxorubicin hydrochloride (DOX). The cumulative drug release from the polymeric micelles showed obvious pH and glucose dependence and was accelerated by slightly decreasing the medium pH or increasing the glucose concentration. *In vitro* antitumor efficiency was evaluated by incubating the DOX loaded micelles with 4T1 breast cancer cells, and the results showed that folate-targeted micelles had higher antitumor activity than the non-targeted ones. Cellular uptake demonstrated by confocal microscopy indicated that free DOX was internalized in the nuclei of 4T1 cells, while the DOX loaded micelles were internalized in the cytoplasm. The cellular uptake of the micelles was enhanced by folate, with stronger fluorescence intensity in the cytoplasm, due to active FR-mediated endocytosis. These folate-conjugated glucose and pH dually responsive micelles may be a potential antitumor drug delivery system for cancer chemotherapy.

Introduction

'Smart' drug delivery systems have attracted much interest from pharmacologists and biomaterials scientists in previous decades, and amphiphilic polymers with the ability to self-assemble into micelles in aqueous solutions are highly promising.[1–4] Advantages of using polymeric micelles as drug carriers include relatively easy structural and functional modification, improved biodistribution and bioavailability of the drugs, and targeted delivery of drugs to correct locations such as tumor cells.[5–8] As most anticancer drugs have poor solubility, high side effects and low bioavailability, the encapsulation of anticancer drugs in polymeric micelles could not only improve the solubility of drugs, but also decrease the risk of multidrug resistance.[9–12] More importantly, the nano-scaled polymeric micelles exhibit tumor accumulation by the enhanced permeability and retention (EPR) effect.[9,13,14] In particular, the microenvironment in a tumor has differences from that of normal tissue. For example, the rate of glucose entry into tumor cells is at least 20–30 fold higher than that in normal cells, because cancer cell growth is heavily dependent on glucose metabolism as a major energy substrate. The interstitial glucose concentration in a tumor ranges from ~15 to 50 mM and varies with type of cancer cell, as well as rate of growth of cancer cells, and the tumor glucose levels even increase to 13–17 fold in hyperglycaemia. Because lactic acid is the final product of glycolysis, the extracellular pH of a solid tumor is lower (6.5–6.8) than normal physiological pH (7.4).[15–18] In addition, many malignant tissues cells, including cancers of the ovary, breast, liver, kidney, uterus, testis, brain, colon and lung, consistently express high levels of specific receptors such as folate receptors (FR-a, FR).[1,19–23] These phenomena have been used to design stimuli triggered polymeric micelles for delivery of anticancer drugs to tumors.

A number of natural or synthetic polymers have been used to form polymeric micelles. Among them, chitosan and its derivatives are the most attractive candidates because of their biochemical activity, biocompatibility, biodegradability and low toxicity and they have been widely used in the pharmaceutical field[15,16,24]. Grafting hydrophobic and hydrophilic segments to the chitosan backbone would give rise to amphiphilic graft copolymers, which could form self-assembled micelles in water. In our previous study, phenylboronic acid grafted chitosan hydrochloride (HCSPBA) was synthesized by coupling amine groups in chitosan hydrochloride with carboxyl groups in 3-carboxyphenylboronic acid. The phenylboronic acid group was introduced as a glucose sensitive moiety, which can be combined with vicinal diol compounds such as glucose to form a more hydrophilic structure. Hydrophobic drugs could be encapsulated by the assembled polymeric micelles of HCSPBA, sustained and glucose responsive drug release was observed as well.[25]

[a]*Faculty of Materials Science and Chemical Engineering, Ningbo University, Ningbo, Zhejiang 315211, P.R. China. E-mail: zhaolingling@nbu.edu.cn*

[b]*Ningbo Key Laboratory of Polymer Materials, Ningbo Institute of Materials Technology and Engineering, Chinese Academy of Sciences, Ningbo, Zhejiang 315201, P.R. China. E-mail: jzhu@nimte.ac.cn; nahaining@nimte.ac.cn*

To enhance intracellular uptake of carriers containing a drug within cancerous cells at the tumor site, it is necessary to develop more effective and active targeting drug delivery systems. A variety of targeting moieties and ligands, such as folate and transferrin, which can substantially increase site-specific targeting, have been immobilized on the surface of drug carriers.[19,26–28] In specific, folate has been utilized as a targeting moiety for enhancing the therapeutic efficacy of many anticancer drugs.[29,30] Folate is a type of small molecular vitamin essential for the combination of the single-carbon metabolism of the eukaryotic cell nucleus and the nuclear glucoside synthesis. It has been reported that the folate receptor (FR) is overexpressed on the surface of several cancers, including breast, kidney, lung, brain, and ovary cancers.[19,20] Folate can bind to FR and facilitate the transfer of folate-targeted micelles through receptor mediated endocytosis. It has been shown that FR has high affinity (K_d >> 10^{-10} M) for folate and mediates the cellular uptake *via* a non-destructive endosomal pathway.[19,27,31] Regarding the limited expression of FR on normal tissues and their overexpression on tumor cells,[19,28,32] folate may be an appropriate choice for targeting tumor cells in micelle-based cancer therapies.

In this study, we designed multifunctional micelles by anchoring the active compounds, phenylboronic acid and folate, to the polymer chain of chitosan hydrochloride. Phenylboronic acid was introduced as a glucose sensitive moiety and folate was conjugated as a targeting moiety, and the synthesized amphiphilic polymer could self-assemble to form glucose and pH dually responsive micelles. DOX was employed as a model anticancer drug and loaded into the polymeric micelles. The characteristics of the micelles, such as particle size and drug release behavior, were studied in detail. In addition, the cytotoxicity of blank and DOX-loaded micelles and the receptor-mediated targeting effect of micelles were evaluated. From the efficient tumor targeting and controlled drug release, it seemed that this system would be of great potential for cancer therapy.

Experimental

Materials

Phenylboronic acid grafted chitosan hydrochloride (HCSPBA) was synthesized according to our previous study,[15,25] the phenylboronic acid content in the HCSPBA unit (mol mol^{-1}) was 0.21, as determined from the C/N ratio by elemental analysis. *N*-Hydroxysuccinimide (NHS) was purchased from Quzhou Xinteng Chemical, China. 1-(3-Dimethylaminopropyl)-3-ethylcarbodiimide hydrochloride (EDC·HCl) was purchased from Sigma Aldrich (St. Louis, US). Folate was purchased from Aladdin Industrial Corporation, China. Pyrene was purchased from Fluka Company (>99%). Doxorubicin hydrochloride (DOX) was purchased from Beijing Huafeng United Technology, China. All the reagents were used as received without further purification. Distilled and deionized water was used in all experiments.

Synthesis of folate modified HCSPBA (FHCSPBA)

FHCSPBA was synthesized by a similar procedure to that previously reported.[22] In brief, HCSPBA (0.1 g) was dissolved in 0.3 wt% acetic acid solution (20 mL) in a 100 mL flask. Folate in 0.05 and 0.2 molar equivalents of HCSPBA unit and NHS (41.6 mg, 0.36 mmol) were dissolved in DMSO (5 mL), and stirred at room temperature for 30 min. To this, EDC·HCl (41.5 mg, 0.22 mmol) was added, and the mixture was stirred to form a uniform solution. Then, the mixed solution of folate/NHS/EDC·HCl was added to the HCSPBA acetic acid solution. After being stirred for 24 h, the mixture was transferred to a dialysis tube with a molecular weight cut-off of 12 kDa and dialyzed against distilled water with one change every 4 h for three days. The dialysate was freeze-dried to harvest yellowish powder-like products (yield, 85–90%). FHCSPBA prepared with theoretical folate grafting ratio of 0.05 and 0.2 were coded as FHCSPBA-I and FHCSPBA-II, respectively. The grafting ratio of folate was determined by fluorescence spectrometry (F-4600, Hitachi factory, Japan) at a wavelength of 450 nm using the calibration curve obtained from folate solutions with different folate concentrations. The excitation wavelength was 370 nm and both excitation and emission bandwidths were set at 10 nm.

Characterization

^{1}H NMR analysis was performed on polymer solutions in D_2O using a Bruker AMX 400 MHz spectrometer. Infrared spectroscopy was tested using a Bruker Equinox 55 spectrometer. Samples were mashed and pressed with KBr and scanned from 4000 to 400 cm^{-1} with a resolution of 2 cm^{-1}. Transmission electron microscopy (TEM) was carried out on a JEM-2100 microscope at an operating voltage of 100 kV. The sample dispersions were dropped onto carbon-coated copper grids and then air-dried. The size distribution of the self-assembled polymeric micelles was performed in aqueous dispersion using a Zetasizer (Nano Series, Malvern Instruments, UK) at 25 °C and repeated three times at a constant concentration of 0.1 mg mL^{-1}.

Measurement of critical micelle concentration (CMC)

The CMC of FHCSPBA was determined using pyrene as a hydrophobic probe in fluorescence spectroscopy.[33] In brief, 200 μL of pyrene in acetone (10^{-5} mol L^{-1}) was added to each of the series of 10 mL vials, acetone was evaporated, 2 mL of various concentrations of FHCSPBA (1×10^{-4} to 0.5 mg mL^{-1}) were added to the vials, and the mixtures were sonicated for 30 min at room temperature. The sample solutions were heated at 37 °C for 24 h to equilibrate pyrene and the micelles, and then left to cool at room temperature. Fluorescence spectra were obtained at the excitation wavelength of 335 nm and the emission wavelength was 360–420 nm for the emission spectra. The excitation and emission bandwidths were set at 5 and 2.5 nm, respectively. Based on the pyrene emission spectra and a decreasing I_{372}/I_{383} with increasing log concentrations of FHCSPBA, the CMC values were calculated by the crossover point at which I_{372}/I_{383} began to decrease rapidly.

Preparation and characterization of DOX-loaded polymeric micelles

DOX loaded polymeric micelles were prepared by a dialysis method. Typically, 10 mg of DOX was dissolved in 5 mL of

methanol and 20 μL of triethylamine was added, and the mixture was stirred for 24 h. Then, the hydrophobic treated DOX solution in methanol was added dropwise to the FHCSPBA solution (20 mg in 10 mL distilled water) under stirring. After being stirred at room temperature for 4 h, the solution was transferred to 12 kDa molecular weight cut-off dialysis tubing and dialyzed for 24 h to remove the organic solvents and free DOX. The solution was freeze-dried to obtain DOX loaded polymeric micelles. The whole procedure was performed in the dark.

The content of encapsulated DOX was determined spectrophotometrically at a wavelength of 490 nm in 0.5 wt% acetic acid using the calibration curve obtained from DOX/0.5 wt% acetic acid solutions with different DOX concentrations. The drug loading content (DLC) and drug loading efficiency (DLE) were calculated according to the following formulas as follows:

$$\text{DLC (wt\%)} = \left[\frac{\text{weight of loaded drug}}{\text{weight of drug loaded micelle}}\right] \times 100$$

$$\text{DLE (\%)} = \left[\frac{\text{weight of loaded drug}}{\text{weight of drug in feeding}}\right] \times 100$$

In vitro release of drug loaded FHCSPBA micelles

In vitro release of DOX from polymeric micelles was conducted using 0.1% (v/v) Tween-80 PBS solution as the dissolution medium with different pH values and glucose concentrations.[16] Typically, DOX loaded polymeric micelles were diluted to 1 mg mL^{-1} in PBS (0.01 M, pH 7.4), and then 1 mL of the solution was transferred into dialysis membrane tubings (Spectra/Por, MWCO 12 kDa). The tubings were immersed into flasks containing 10 mL of release medium as a sink condition (37 °C). At desired time intervals, 2 mL of released medium was taken out and replenished with an equal volume of fresh medium. The amount of released DOX was detected by a fluorescence detector with excitation wavelength at 494 nm and emission wavelength at 594 nm. The release experiments were conducted in triplicate and the results were presented as the average data with standard deviations.

Cytotoxicity assay

L929 fibroblasts were cultured in Dulbecco's Modified Eagle's Medium (DMEM) supplemented with 10% fetal bovine serum, 100 μg mL^{-1} streptomycin and 100 IU mL^{-1} penicillin. The temperature of the incubator was set to 37 °C under a humidified atmosphere containing 5% CO_2.

The relative cytotoxicity of FHCSPBA micelles was obtained by Cell Counting Kit-8 (CCK-8) assay against L929 fibroblasts. The cells were seeded onto 96-well plates at a density of 4×10^4 cells per well in 100 μL of medium. After 24 h incubation, the culture medium was removed and replaced with 100 μL of medium containing FHCSPBA micelles of different concentrations. The cells were incubated for another 24 h. The culture medium was removed and the wells were rinsed with PBS (pH 7.4) three times. Then, 100 μL of DMEM containing 10 μL of CCK-8 solution was added to each well and incubated for another 2 h. The absorbance of each well was measured at 450 nm using a microplate reader (Thermo MULTISKAN MK3). Cell viability was calculated by the following equation.

$$\text{Cell viability (\%)} = \frac{\text{Int}_s}{\text{Int}_{control}} \times 100$$

where Int_s is the absorbance intensity of the cells incubated with the samples and $Int_{control}$ is the absorbance intensity of the cells incubated with the culture medium only.

In vitro anticancer efficiency of drug loaded micelles

The *in vitro* anticancer efficiency of drug loaded polymeric micelles against 4T1 breast cancer cells was evaluated by CCK-8 assay. Approximately 4×10^4 cells per well were seeded in 96-well plates with 100 μL of DMEM medium for 24 h before the tests. DOX and DOX loaded polymeric micelles with different concentrations (from 0.001 to 500 μg mL^{-1}) in DMEM were added to the medium of 96-well plates and incubated for 24 h. The culture medium was removed and the wells were rinsed with PBS three times. Subsequently, CCK-8 assay was conducted as described above. The half maximal inhibitory concentration (IC50) of the micelles and DOX were calculated using SPSS software ($n = 3$).

Cellular uptake of drug loaded micelles

Confocal laser scanning microscopy (CLSM) was employed to evaluate the qualitative cellular uptake of the DOX loaded micelles. The 4T1 cells were seeded onto 35 mm diameter glass dishes at a density of 4×10^4 cells per well. After incubation in DMEM with 10% FBS and 5% CO_2 at 37 °C for 24 h, when the 4T1 cells were at a logarithm phase, 250 μL of DMEM solution of DOX or DOX loaded micelles were added into the wells with the DOX concentration of 50 μg mL^{-1}. The 4T1 cells were incubated at 37 °C for another 3 h before the culture medium was removed and the dishes were rinsed with PBS three times. The cell nucleus was stained with DAPI for 20 min and washed with PBS. In the control group, the 4T1 cells were incubated with excess free folate (2 mM) for 4 h before the DOX and DOX loaded micelles were added, whereas the other conditions were kept the same. CLSM images of cells were observed using a FV 1000-IX81 confocal laser scanning microscope (Olympus, Japan), with an excitation wavelength of 405 nm and 488 nm and emission wavelength of 425–475 nm for DAPI and 500–580 nm for DOX.

Results and discussion

Synthesis and characterization of FHCSPBA

The synthetic routes of amphiphilic FHCSPBA are illustrated in Scheme 1a. The two small molecules of phenylboronic and folate were immobilized on the chitosan hydrochloride (HCS) by the coupling reaction of $-NH_2$ in HCS with –COOH in PBA and folate. The structures of the graft polymers were characterized by ^1H NMR and FTIR spectra. As shown in the ^1H NMR

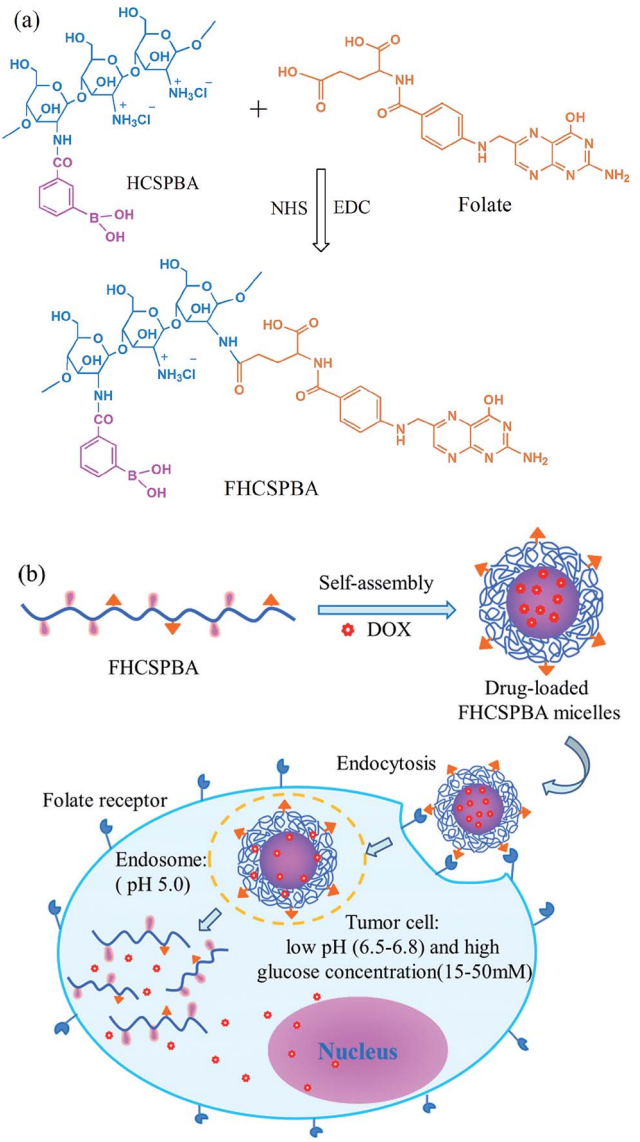

Scheme 1 Illustrative synthesis of FHCSPBA (a), and the formation of drug-loaded micelles, take up of the micelles by tumor cells and drug release in response to a range of stimuli characteristic of tumor tissues and intracellular microenvironments (b).

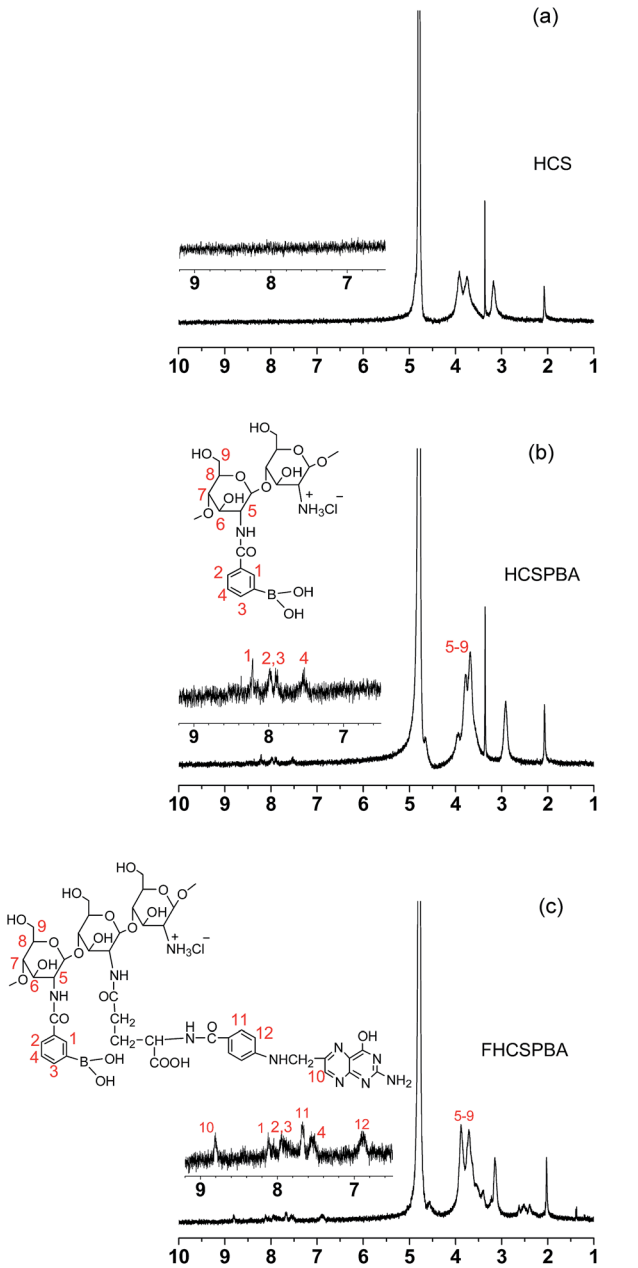

Fig. 1 ^{1}H NMR spectra of HCS (a), HCSPBA (b) and FHCSPBA (c).

spectrum (Fig. 1), the broad peak at $\delta = 3.6$ ppm is assigned to the protons on C2–C6 of the HCS unit. Peaks at $\delta = 7.4$, 7.8, and 8.2 ppm are assigned to proton signals on the benzene ring of PBA, the peak at $\delta = 2.9$ ppm is from methylene protons of succinic acid on the HCS backbone, and the peak at $\delta = 2.0$ ppm corresponds to the protons of CH_3 on the nondeacylated CONH content.[15,25] The new signals at $\delta = 6.8$, 7.6 and 8.9 ppm in FHCSPBA are assigned to protons on the benzene and pteridine rings of folate.[1,34] The FTIR spectrum of FHCSPBA shows an increased peak at 1564 cm^{-1} relative to that of the HCSPBA spectrum (Fig. 2). This peak is usually caused by secondary amines, suggesting that the substitution of the amino groups in HCSPBA was increased. Comparing the FTIR spectra of folate with that of FHCSPBA, the absorption band at 1729 cm^{-1}, the specific peak of carbonyl groups, testifies to the presence of the –NHCOCHCOOH– group in folate, and the appearance of the peak at 1608 cm^{-1} in the spectrum of FHCSPBA is attributed to the benzene ring of the folate.[22,35]

The graft amount of folate in FHCSPBA could be tuned by changing the feeding molar ratio of the HCSPBA unit to folate and was determined by fluorescence spectrometry. The results show that the graft amount increases with the increase of folate amount, as shown in Table 1. The content of folate in the FHCSPBA unit was much lower than the feeding ratio; it was 1/36 and 1/9 when the feeding molar ratio of folate to HCSPBA unit was 0.05 and 0.2, respectively.

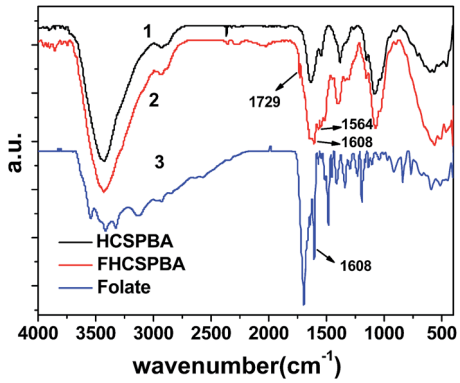

Fig. 2 FTIR spectra of HCSPBA (1), FHCSPBA (2) and folate (3).

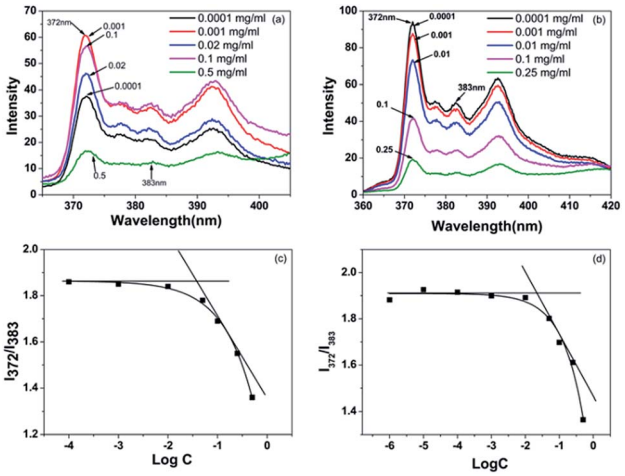

Fig. 3 Pyrene emission spectra of FHCSPBA-I (a) and FHCSPBA-II (b) solution (excitation wavelength of 335 nm). The intensity ratio (I_{372}/I_{383}) of the pyrene emission *versus* the log concentration of FHCSPBA-I (c) and FHCSPBA-II (d).

Characterizations of blank and drug loaded polymeric micelles

Both HCSPBA and FHCSPBA can self-assemble in PBS due to their amphiphilic natures. The CMC was determined using a fluorescence spectrophotometer with pyrene as the probe. At low concentration (C) of FHCSPBA (C < CMC), there are small or negligible changes in the fluorescence intensity ratio of I_{372}/I_{383}. As the concentration is increased, remarkable decrease of the intensity ratio (I_{372}/I_{383}) is observed (Fig. 3). Fig. 3b and d shows the intensity ratio (I_{372}/I_{383}) of the pyrene excitation spectra *versus* the log concentrations of FHCSPBA-I and FHCSPBA-II, respectively. Based on the intensity ratio data, the CMC value of FHCSPBA was calculated from the crossover point.[24,34] All the CMC values of FHCSPBA with different folate content were listed in Table 1. As show in Table 1, the CMC of HCSPBA is 0.020 mg mL^{-1} and the CMC of FHCSPBA is 0.033 and 0.053 mg mL^{-1} with a folate content of 1/36 and 1/9, respectively. Spherical aggregates were observed by TEM, as shown in Fig. 4. The size of the polymeric micelles measured by DLS decreases with increasing folate content and the values are 334 ± 13, 237 ± 55 and 187 ± 10 nm for HCSPBA, FHCSPBA-I and FHCSPBA-II, respectively, which are much larger than micelles formed from low molecular weight surfactants and thus implies a multicore structure of the aggregates.[25,33]

DOX was used as a model anticancer drug to evaluate the loading and release properties of the FHCSPBA micelles. DOX is widely used to treat various solid malignant tumors by interacting with DNA by way of intercalation and inhibition of macromolecular biosynthesis. The drug loading content (DLC) and drug loading efficiency (DLE) of the polymeric micelles were tested spectro-photometrically at a wavelength of 490 nm (Table 1). The DLC and DLE of FHCSPBA micelles were lower than those of HCSPBA micelles, which may have been caused by the variation of the solubility and electron charge of FHCSPBA, which thus affected the DOX loading of the polymeric micelles. The morphologies of blank and drug loaded micelles were shown in Fig. 4. After loading with DOX, the size of the micelles increased significantly due to the solubilizing of hydrophobic treated DOX into the polymeric micelles.[25,36] As show in Fig. 5, the sizes of DOX-loaded micelles increased from 362 ± 11 to 875 ± 27 nm and 187 ± 10 to 720 ± 85 nm, tested by DLS, for FHCSPBA-I and FHCSPBA-II, respectively.

The phenomenon of size change with change in pH value or glucose concentration was reported in some pH- or glucose-sensitive nanocarriers.[24,25] In this study, the phenomenon of pH and glucose dependent size change was also observed. The phenylboronic acid group can combine with glucose to form a hydrophilic complex in the presence of glucose and the charge repulsion of FHCSPBA is increased at low pH, resulting in the swelling or collapse of FHCSPBA micelles. DLS measurements verified that the size of blank FHCSPBA-I micelles in pH 7.4 solution was 362 ± 11 nm and increased to 633 ± 65 nm obviously in pH 6.5 and then slightly increased to 686 ± 37 nm

Table 1 Folate content, CMC of FHCSPBA, particle size, drug loading content and drug loading efficiency of polymeric micelles

Sample	Folate feed ratio (folate/HCSPBA unit, mol mol^{-1})	Folate graft ratio[a] (folate/FHCSPBA unit, mol mol^{-1})	CMC[b] (mg mL^{-1})	DLC (wt%)	DLE (%)	Particle size[c] (nm)
HCSPBA	0	0	0.020	25.3%	65.6%	334 ± 13
FHCSPBA-I	1 : 20	1 : 36	0.033	14.6%	36.4%	237 ± 55
FHCSPBA-II	1 : 5	1 : 9	0.053	19.6%	56.1%	187 ± 10

[a] Determined by fluorescence spectrometry. [b] Determined by I_{372}/I_{383} ratio (I_1/I_3) of pyrene fluorescence emission as a function of polymer concentration. [c] Mean value measured using DLS.

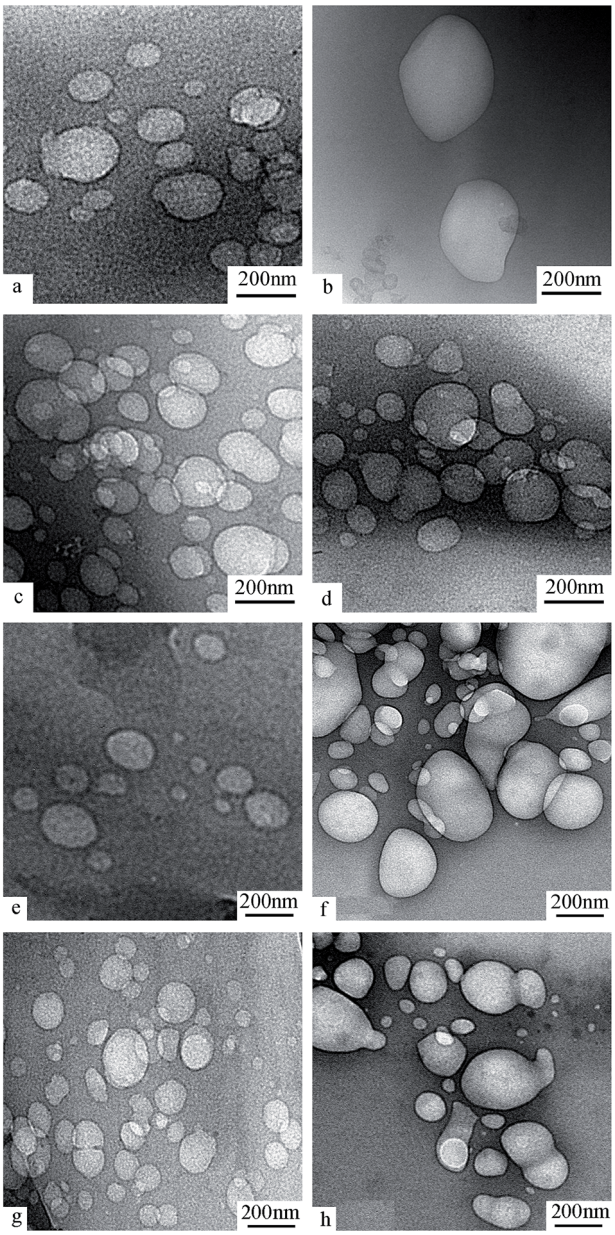

Fig. 4 TEM images of FHCSPBA-I micelles (a) and DOX loaded FHCSPBA-I micelles (b) at pH 7.4, FHCSPBA-I micelles at pH 5.0 (c) and pH 7.4 with 50 mM glucose (d); FHCSPBA-II micelles (e) and DOX loaded FHCSPBA-II micelles (f) at pH 7.4, FHCSPBA-II micelles at pH 5.0 (g) and pH 7.4 with 50 mM glucose (h).

in pH 5.0, as shown in Fig. 6a. The size of blank FHCSPBA-I micelles also increased with the glucose concentration of the medium; the value increased to 487 ± 53 and 503 ± 19 nm at glucose concentration of 25 and 50 mM, respectively (Fig. 6b). The size change of blank FHCSPBA-II micelles showed pH and glucose sensitivity as well; the size increased to 618 ± 88 and 643 ± 98 nm in pH 6.5 and 5.0, respectively, from 187 ± 10 nm in pH 7.4 (Fig. 6c). The values were 411 ± 36 and 496 ± 31 nm at glucose concentration of 25 and 50 mM, respectively (Fig. 6d). As shown in the TEM images (Fig. 4), the polymeric micelles swelled but did not collapse in lower pH and high glucose

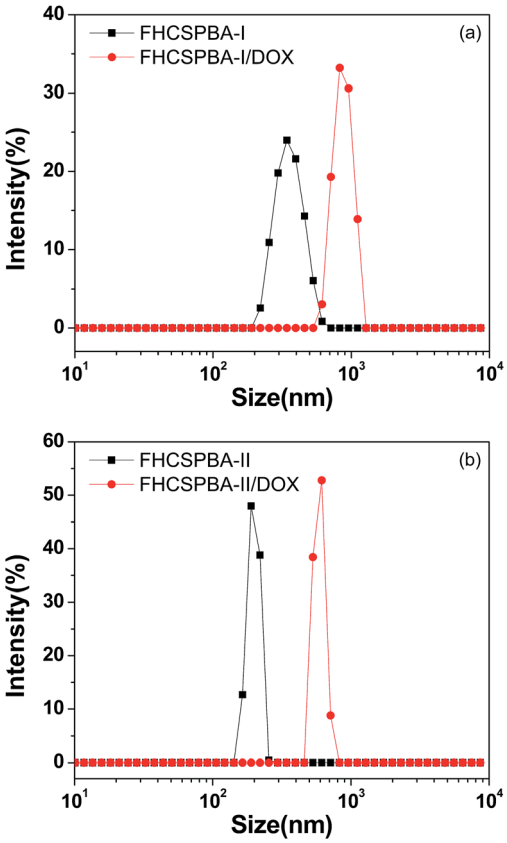

Fig. 5 Size distribution of blank and drug loaded FHCSPBA-I (a) and FHCSPBA-II (b) micelles.

concentration and they retained spherical morphologies. These results indicate that the micelles formed by FHCSPBA are highly sensitive to acidic pH and glucose, which is favorable for targeting delivery in tumor treatment because of the low pH and high glucose concentration in tumor tissues.

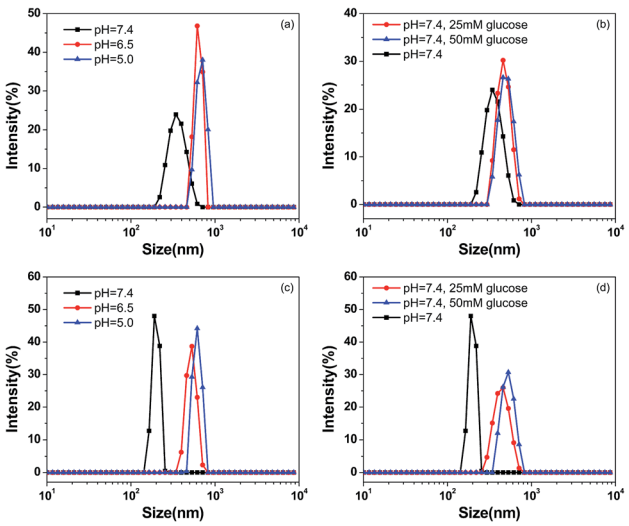

Fig. 6 Size distribution of blank FHCSPBA-I (a and b) and FHCSPBA-II (c and d) micelles at different pH values and glucose concentrations.

In vitro drug release

The drug release of DOX loaded micelles was investigated at 37 °C in PBS containing 0.1% (v/v) Tween-80 with different pH values and glucose concentrations. Sustained drug release from the drug loaded polymeric micelles was observed without initial burst release (Fig. 7), and the drug release was accelerated by either decreasing the medium pH or increasing the glucose concentration, due to the swelling of the FHCSPBA micelles. As demonstrated in Fig. 7a, the drug release from FHCSPBA-II micelles was very slow at physiological pH (7.4), and the cumulative release of DOX was 31.5% at a release time of 170 h. When the medium pH was low, the electrostatic repulsion of FHCSPBA increased due to the protonation of amino groups, resulting in the swelling of FHCSPBA micelles and accelerating drug release from the micelles. The cumulative release of DOX increased to 44.4% and 78.7% at a release time of 170 h at tumor pH (6.5) and lysosome pH (5.0), respectively. The DOX release was also accelerated in the presence of glucose due to the more hydrophilic forms of FHCSPBA micelles after the phenylboronic acid groups combined with glucose and the cumulative release of DOX was 43.6% and 87.8% at a release time of 170 h at physiological pH (7.4) with 25 mM and 50 mM glucose, respectively. The drug release from the polymeric micelles with low folate content demonstrated similar pH and glucose dependence. As demonstrated in Fig. 7b, the cumulative release of DOX from FHCSPBA-I micelles was 23.0% at a release time of 170 h at physiological pH (7.4), and the value increased to 59.4% and 80.3% at tumor pH (6.5) and lysosome pH (5.0), respectively. The presence of glucose could also accelerate the drug release and the cumulative release of DOX was 48.6% and 93.8% at a release time of 170 h at physiological pH (7.4) with 25 mM and 50 mM glucose, respectively. For the low pH and high glucose concentration microenvironment in tumor tissue, the pH and glucose sensitivity of DOX release from the drug loaded FHCSPBA micelles should be beneficial for the system applied in tumor treatment.[15,37]

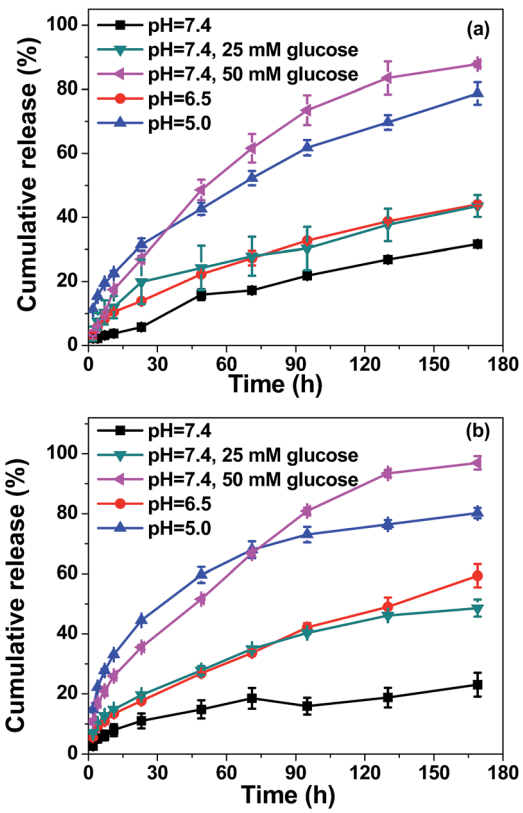

Fig. 7 Cumulative release of DOX from the drug loaded FHCSPBA-II (a) and FHCSPBA-I (b) micelles immersed in 10 mL of saline in different media.

The biocompatibility of micelles

To investigate the cytotoxicity of polymeric micelles, L929 fibroblasts with medium containing blank micelles at different concentrations (10–1000 μg mL^{-1}) were evaluated using Cell Counting Kit-8 (CCK-8) assay. The results were presented in Fig. 8; the cell viability decreased as the micelle concentration increased, but the relative cell viability was higher than 90% even when the concentration was as high as 1 mg mL^{-1}. Thus, no obvious growth inhibition effect was found after incubation with the blank micelles even at the highest concentration at 1 mg mL^{-1} for 24 h, indicating that the polymers with different folate content were nontoxic as nanocarriers. The results suggest that the newly developed FHCSPBA are biocompatible and suitable for biomedical applications.

In vitro anticancer efficiency

To evaluate whether the FHCSPBA micelles are efficient carriers for anticancer drug delivery, the *in vitro* anticancer activity of drug loaded micelles was measured. DOX loaded micelles were incubated with 4T1 breast cancer cells, and free DOX was used as control. As shown in Fig. 9, significant proliferation inhibition of cells following 24 h incubation with DOX loaded micelles was observed. The IC50 of drug loaded micelles was 18.0, 16.4 and 23.1 μg mL^{-1} for DOX loaded HCSPBA, FHCSPBA-I and FHCSPBA-II micelles, respectively, and much higher than that of free DOX (0.57 μg mL^{-1}). It seems that free DOX showed higher toxicity to cells than the micelle formulations due to its higher and nonspecific cellular uptake, but the effect lessened with time due to the generation of drug resistance of cells.

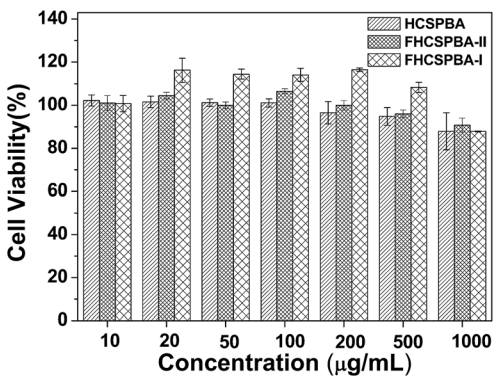

Fig. 8 Viability of L929 cells after being incubated with DOX-free micelles at different concentrations for 24 h ($n = 3$).

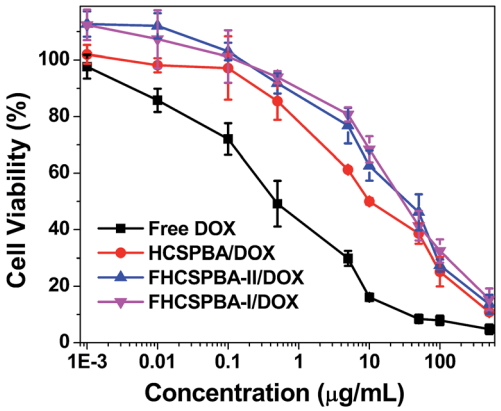

Fig. 9 Anticancer activity of DOX loaded HCSPBA micelles, DOX loaded FHCSPBA micelles and free DOX as a function of concentration. The cells were incubated against 4T1 cells with DOX-loaded micelles or free DOX for 24 h.

Because DOX is a small molecule and hydrophilic, and it is internalized in cells easily and directly *via* pinocytosis.[9,38] The intracellular transportation of polymeric micelles may not be as fast or efficient as the direct diffusion of free DOX and resulted in greater cell viability. However, nano- or sub-micrometer sized drug formulations can be internalized by endocytosis[9,39] and this can be further enhanced by installing targeting ligands, such as folate, aptamer, peptide, and antibody moieties, that facilitate efficient and specific cellular uptake of micelles.[40] The IC50 of DOX-loaded HCSPBA micelles is 4.6 μg DOX equiv. mL^{-1} for 4T1 cells after 24 h of incubation. Therefore, the polymer formulations are still considered to be toxic to cancer cells and the anticancer activity of DOX-loaded polymeric micelles can be enhanced by installing folate as a targeting ligand. The IC50 of DOX-loaded FHCSPBA-I and FHCSPBA-II micelles are 2.6 and 3.5 μg DOX equiv. mL^{-1} for 4T1 cells, respectively, calculated based on Fig. 9, which were lower than that obtained with the non-folate HCSPBA counterpart under otherwise the same conditions.

In vitro cellular uptake

CLSM was applied to investigate the cellular uptake behavior and intracellular distribution of DOX loaded micelles and free DOX in 4T1 cells. After a predetermined interval of 3 h, the nuclei were stained by DAPI and observed by confocal microscopy. The results revealed that the uptake of free DOX by cell nuclei was crucial and they showed red fluorescence only in the nucleus, because DOX has to intercalate with DNA to induce cell death.[40,41] In contrast, weaker DOX fluorescence was observed for 4T1 cells incubated with DOX-loaded HCSPBA and FHCSPBA micelles under otherwise the same conditions and the red fluorescence mainly originated from the cytoplasm (Fig. 10), because the DOX-loaded micelles were internalized *via* endocytosis, while free DOX was internalized *via* diffusion.[9] The folate-enhanced delivery of micelles was also observed. It was found that in Fig. 10, cells incubated with the folate-targeted micelles (FHCSPBA-I and FHCSPBA-II) showed much stronger

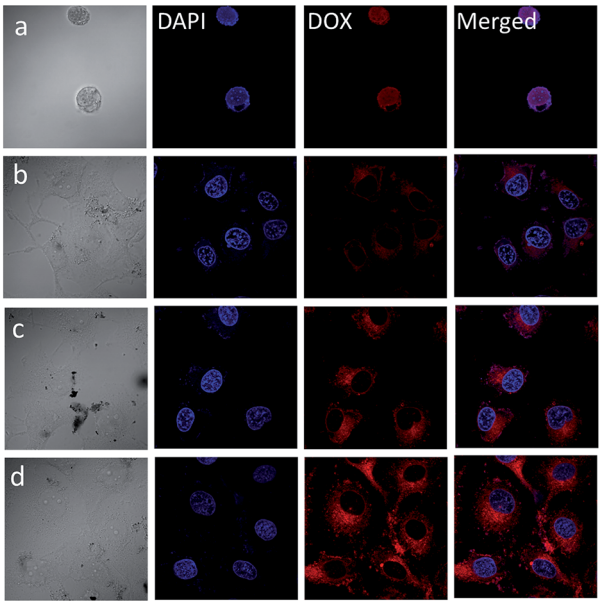

Fig. 10 CLSM images of 4T1 cells incubated with free DOX (a), DOX loaded HCSPBA micelles (b), DOX loaded FHCSPBA-I micelles (c) or DOX loaded FHCSPBA-II micelles (d) for 3 h (DOX concentration was 50 μg mL^{-1}). Cell nuclei were stained with DAPI.

DOX fluorescence in comparison with cells incubated with the non-targeted ones (HCSPBA). The weaker fluorescence of DOX-loaded HCSPBA micelles might be explained by the slightly slower cellular uptake from that of DOX-loaded FHCSPBA micelles, and the strong fluorescence intensity in the cytoplasm

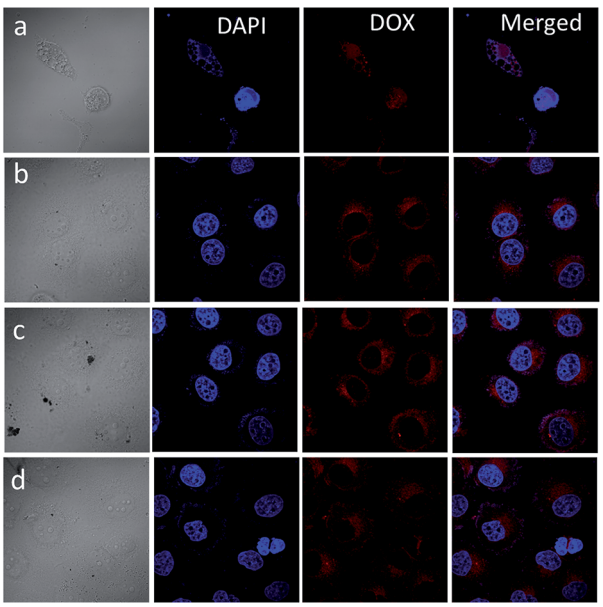

Fig. 11 CLSM images of 4T1 cells were first incubated with excess folate for 4 h and then with free DOX (a), DOX loaded HCSPBA micelles (b), DOX loaded FHCSPBA-I micelles (c) or DOX loaded FHCSPBA-II micelles (d) for 3 h (DOX concentration was 50 μg mL^{-1}). Cell nuclei were stained with DAPI.

is a result of active FR-mediated endocytosis.[21,42] To further confirm this, the 4T1 cells were incubated first with an excess amount of folate for 4 h to interrupt the FA-receptor interaction between the micelles and the cell membrane, and then free DOX and DOX loaded micelles were added to the wells for another 3 h of incubation. Compared with the stronger DOX fluorescence of folate-targeted micelles (FHCSPBA) than that of non-targeted ones (HCSPBA), the intensity of DOX fluorescence showed no significant difference between them when excess folate was added, as shown in Fig. 11. The result indicated that the internalization of the folate-containing FHCSPBA micelles could be significantly inhibited by the addition of free folate molecules, which suggests the selectivity of transportation of the FHCSPBA micelles to FA-receptor expressing cells through an active FR-mediated endocytosis pathway. The result is in agreement with the *in vitro* anticancer efficiency test result, wherein the FHCSPBA micelles have lower IC50 (DOX equiv. mL^{-1}) and higher anticancer activity than the non-folate micelles due to the efficient and specific cellular uptake of micelles facilitated by folate as a targeting ligand.

Conclusions

Folate-conjugated, glucose and pH dual-responsive micelles were developed by anchoring phenylboronic acid and folate to the polymer chain of chitosan hydrochloride and the blank micelles showed non-cytotoxicity. DOX was employed as an anticancer drug model and loaded into the polymeric micelles. Sustained glucose and pH dually sensitive drug release from the drug loaded micelles was observed and the cumulative drug release could be accelerated by slightly decreasing the medium pH or increasing the glucose concentration. *In vitro* anticancer efficiency and cell uptake were evaluated by incubating the DOX loaded micelles with 4T1 breast cancer cells and the results showed that folate-targeted micelles (FHCSPBA) had higher anticancer activity than non-targeted ones (HCSPBA). Free DOX was internalized into the nuclei of 4T1 cells *via* diffusion, whereas the DOX loaded micelles were internalized in the cytoplasm *via* endocytosis, and the cellular uptake of the micelles was enhanced by folate, with stronger fluorescence intensity in the cytoplasm. Because of the different microenvironments (low pH, high glucose concentration and over-expression of folate receptor) in cancer cells, these folate-conjugated glucose and pH dually responsive micelles appear to be a promising platform for targeted anticancer drug release.

Acknowledgements

This study is financially sponsored by the National Natural Science Foundation of China (51403108), the Natural Science Foundation of Zhejiang Province, China (LQ13B040001), the Open Fund of Beijing National Laboratory for Molecular Sciences, the Open Fund of Zhejiang Provincial Top Key Discipline of Aquaculture and K. C. Wong Magna Fund in Ningbo University.

References

1 S. Hassanzadeh, Z. Feng, T. Pettersson and M. Hakkarainen, *Polymer*, 2015, **74**, 193.
2 S. Lee, H. Kim, S. Chae and B. H. Sohn, *Polymer*, 2015, **61**, 15.
3 Z. Chen, P. A. FitzGerald, Y. Kobayashi, K. Ueno, M. Watanabe, G. G. Warr and R. Atkin, *Macromolecules*, 2015, **48**, 1843.
4 Y. Singh and M. P. Palombo, *Curr. Med. Chem.*, 2008, **15**, 1802.
5 Y. K. Jung, M. H. Park, H. J. Moon, U. P. Shinde and B. Jeong, *Macromolecules*, 2013, **46**, 4215.
6 L. Jiang, Z. M. Gao, L. Ye, A. Y. Zhang and Z. G. Feng, *Polymer*, 2013, **54**, 5188.
7 J. Hu, J. He, M. Zhang and P. Ni, *J. Controlled Release*, 2015, **213**, e86.
8 C. Deng, Y. Jiang, R. Cheng, F. Meng and Z. Zhong, *Nano Today*, 2012, **7**, 467.
9 Y. Lei, Y. Lai, Y. Li, S. Li, G. Cheng, D. Li, H. Li, B. He and Z. Gu, *Int. J. Pharm.*, 2013, **453**, 579.
10 X. Li, P. Li, Y. Zhang, Y. Zhou, X. Chen, Y. Huang and Y. Liu, *Pharmaceut. Res.*, 2010, **27**, 1498.
11 X. B. Xiong, Y. Huang, W. L. Lu, X. Zhang, H. Zhang, T. Nagai and Q. Zhang, *J. Controlled Release*, 2005, **107**, 262.
12 J. Makino, H. Cabral, Y. Miura, Y. Matsumoto, M. Wang, H. Kinoh, Y. Mochida, N. Nishiyama and K. Kataoka, *J. Controlled Release*, 2015, **220**, 783.
13 S. Acharya and S. K. Sahoo, *Adv. Drug Delivery Rev.*, 2011, **63**, 170.
14 V. Torchilin, *Adv. Drug Delivery Rev.*, 2011, **63**, 131.
15 J. Li, W. Hu, Y. Zhang, H. Tan, X. Yan, L. Zhao and H. Liang, *J. Polym. Sci., Part A: Polym. Chem.*, 2015, **53**, 1235.
16 L. Zhao, L. Zhu, F. Liu, C. Liu, Shan-Dan, Q. Wang, C. Zhang, J. Li, J. Liu, X. Qu and Z. Yang, *Int. J. Pharm.*, 2011, **410**, 83.
17 U. Kedar, P. Phutane, S. Shidhaye and V. Kadam, *Nanomedicine*, 2010, **6**, 714.
18 A. Kumar, N. K. Vishvakarma, A. Tyagi, A. C. Bharti and S. M. Singh, *Biosci. Rep.*, 2011, **32**, 91.
19 B. Bahrami, M. Mohammadnia-Afrouzi, P. Bakhshaei, Y. Yazdani, G. Ghalamfarsa, M. Yousefi, S. Sadreddini, F. Jadidi-Niaragh and M. Hojjat-Farsangi, *Tumor Biol.*, 2015, **36**, 5727.
20 G. Hong, R. Yuan, B. Liang, J. Shen, X. Yang and X. Shuai, *Biomed. Microdevices*, 2008, **10**, 693.
21 H. Zhao, H. H. P. Duong and L. Y. L. Yung, *Macromol. Rapid Commun.*, 2010, **31**, 1163.
22 H. Zhu, F. Liu, J. Guo, J. Xue, Z. Qian and Y. Gu, *Carbohydr. Polym.*, 2011, **86**, 1118.
23 P. J. Kinnari, M. L. Hyvönen, E. M. Mäkilä, M. H. Kaasalainen, A. Rivinoja, J. J. Salonen, J. T. Hirvonen, P. M. Laakkonen and H. A. Santos, *Biomaterials*, 2013, **34**, 9134.
24 J. Liu, H. Li, X. Jiang, C. Zhang and Q. Ping, *Carbohydr. Polym.*, 2010, **82**, 432.
25 Y. Zhang, J. Zheng, J. Li, W. Hu, Y. Sun, H. Liang, L. Zhao and F. Liang, *Acta Polym. Sin.*, 2015, **9**, 1020.

26 Z. Du, S. Pan, Q. Yu, Y. Li, Y. Wen, W. Zhang, M. Feng and C. Wu, *Colloids Surf., A*, 2010, **353**, 140.
27 G. A. Mansoori, K. S. Brandenburg and A. Shakeri-Zadeh, *Cancers*, 2010, **2**, 1911.
28 W. Ye, J. Du, B. Zhang, R. Na, Y. Song, Q. Mei, M. Zhao and S. Zhou, *PLoS One*, 2014, **9**, e97358.
29 S. Khoee and A. Kavand, *Eur. J. Med. Chem.*, 2014, **73**, 18.
30 K. Yao, J. Wang, C. Wang, C. Tang and X. Jiang, *J. Mater. Chem. B*, 2013, **1**, 2324.
31 S. K. Murthy, *Int. J. Nanomed.*, 2007, **2**, 129.
32 N. Parker, M. J. Turk, E. Westrick, J. D. Lewis, P. S. Low and C. P. Leamon, *Anal. Biochem.*, 2005, **338**, 284.
33 L. Zhu, L. Zhao, X. Qu and Z. Yang, *Langmuir*, 2012, **28**, 11188.
34 T. Lu, J. Sun, X. Chen, P. Zhang and X. Jing, *Macromol. Biosci.*, 2009, **9**, 1059.
35 N. Aoki, M. Nishikawa and K. Hattori, *Carbohydr. Polym.*, 2003, **52**, 219.
36 Y. Yang, Y. Guo, R. Sun and X. Wang, *Carbohydr. Polym.*, 2016, **145**, 56.
37 U. Manna and S. Patil, *ACS Appl. Mater. Interfaces*, 2010, **2**, 1521.
38 L. Luo, J. Tam, D. Maysinger and A. Eisenberg, *Bioconjugate Chem.*, 2002, **13**, 1259.
39 I. Canton and G. Battaglia, *Chem. Soc. Rev.*, 2012, **41**, 2718.
40 W. Chen, P. Zhong, F. Meng, R. Cheng, C. Deng, F. Jan and Z. Zhong, *J. Controlled Release*, 2013, **169**, 171.
41 D. A. Gewirtz, *Biochem. Pharmacol.*, 1999, **57**, 727.
42 Y. Sun, Y. Li, S. Nan, L. Zhang, H. Huang and J. Wang, *J. Colloid Interface Sci.*, 2015, **458**, 119.